

**QCD Test in Three Jet  $Z^0$  Decays at SLD and Detector Development for  
 $H^0 \rightarrow \text{Gamma Gamma}$  Searches in High Energy Hadron Colliders \***

Hyun Hwang

Stanford Linear Accelerator Center  
Stanford University  
Stanford, CA 94309

SLAC-Report-689  
August 1994

Prepared for the Department of Energy  
under contract number DE-AC03-76SF00515

Printed in the United States of America. Available from the National Technical Information Service, U.S. Department of Commerce, 5285 Port Royal Road, Springfield, VA 22161.

---

\* Ph.D. thesis, University of Oregon, Eugene, OR 97403

QCD TEST IN THREE-JET  $Z^0$  DECAYS AT SLD AND DETECTOR  
DEVELOPMENT FOR  $H^0 \rightarrow \gamma\gamma$  SEARCHES IN HIGH ENERGY  
HADRON COLLIDERS

by

HYUN HWANG

A DISSERTATION

Presented to the Department of Physics  
and the Graduate School of the University of Oregon  
in partial fulfillment of the requirements  
for the degree of  
Doctor of Philosophy

August 1991

"QCD Test in Three-Jet  $Z^0$  Decays at SLD and Detector Development for  $H^0 \rightarrow \gamma\gamma$  Searches in High Energy Hadron Colliders," a dissertation prepared by Hyun Hwang in partial fulfillment of the requirements for the Doctor of Philosophy degree in the Department of Physics. This dissertation has been approved and accepted by:

*James E. Brau*

---

Dr. James E. Brau, Chair of the Examining Committee

*August 20, 1994*

Date

Committee in charge: Dr. James E. Brau, Chair  
Dr. Raymond E. Frey  
Dr. Nilendra G. Deshpande  
Dr. Kwangjai Park  
Dr. James Isenberg

Accepted by:

*[Signature]*

---

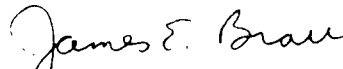
Vice Provost and Dean of the Graduate School

## An Abstract of the Dissertation of

Hyun Hwang for the degree of Doctor of Philosophy  
 in the Department of Physics to be taken August 1994

Title: QCD TEST IN THREE-JET  $Z^0$  DECAYS AT SLD AND DETECTOR  
 DEVELOPMENT FOR  $H^0 \rightarrow \gamma\gamma$  SEARCHES IN HIGH ENERGY  
 HADRON COLLIDERS

Approved: \_\_\_\_\_



Dr. James E. Brau

Polarized  $Z^0$  decays into three jets have been detected and measured in the SLD (SLAC Large Detector) experiment at the Stanford Linear Accelerator Center (SLAC). The hadrons from the jets were detected in the SLD liquid argon calorimeter, providing a sensitivity over 98% of the solid angle. The spin of the gluon was tested by studying the scaled jet energies ( $x_1, x_2, x_3$ ), the Ellis-Karliner angle ( $\cos\theta_{EK}^*$ ) and the parameters of event plane orientation ( $\alpha, \alpha_N, \chi$ ). These measured variables are compared with quantum chromodynamics (QCD) and a scalar gluon model. Good agreement is found between data and the vector QCD model for the distributions of  $x_1, x_2, x_3$  and  $\cos\theta_{EK}^*$ .

Two detector prototypes for the GEM detector of the Superconducting Super Collider have been studied: a prototype silicon-tungsten preradiator and a liquid

argon hadron calorimeter. The silicon-tungsten preradiator was designed for the GEM detector to distinguish between single photons from Higgs decay and background photon pairs from  $\pi^0$  decay. This preradiator was tested in a beam at Brookhaven National Laboratory in July, 1992. A lead glass array placed behind the silicon was used to determine energy resolution effects. The results from the test on spatial distributions and energy resolution<sup>3</sup>, including correction for the energy deposited in the preradiator are presented, along with comparisons to EGS simulations. Data from a beam test of the liquid argon prototype was analyzed and compared to CALOR89 simulations. The studies concentrated on energy resolution optimization and electronic noise suppression.

## CURRICULUM VITA

NAME OF AUTHOR: Hyun Hwang

PLACE OF BIRTH: Seoul, Republic of Korea

DATE OF BIRTH: August 6, 1954

### GRADUATE AND UNDERGRADUATE SCHOOLS ATTENDED:

University of Oregon  
University of Arizona  
Sogang University

### DEGREES AWARDED:

Doctor of Philosophy in Physics, 1994, University of Oregon  
Master of Science in Physics, 1987, University of Arizona  
Bachelor of Arts in Physics, 1978, Sogang University

### AREAS OF SPECIAL INTEREST:

Experimental High Energy Physics

### PROFESSIONAL EXPERIENCE:

Research Assistant, Department of Physics, University of Oregon, Eugene, 1989-91

Teaching Assistant, Department of Physics, University of Arizona, Tucson, 1985-87

Researcher, Korean Chemical Research Institute, Seoul, Korea, 1983-84

### PUBLICATIONS:

1. A. Arodzero *et al.*, IEEE Transactions on Nuclear Science, Vol.40, No.4, August 1993.

2. S.C. Berridge *et al.*, IEEE Trans. Nucl. Sci. 39, 1242 (1992).
3. Koichiro Furuno *et al.*, "Neutron Flux Suppression with Polyethylene Moderators in the EMPACT Silicon EM Calorimeter", in SSC *R&D* Symposium Fort Worth, Texas Oct. 15-18, 1990.
4. R. Korde *et al.*, "Low Cost, Large Area Silicon Detectors for Calorimetry", in SSC *R&D* Symposium Fort Worth, Texas Oct. 15-18, 1990.

## ACKNOWLEDGMENTS

I personally appreciate my advisor, James Brau, for his guidance, encouragement and patience. I also wish to appreciate Raymond Frey and David Strom for their advice.

I would especially like to thank the members of the University of Oregon Luminosity Group: Koichiro Furuno, Kevin Pitts, Matt Langston, Anatoli Arodzero, Xiao Qing Yang, Hwanbae Park, J. Zhou and David Mason. I especially wish to thank for Kevin Pitts's help.

I also appreciate Philip Burrows for his help as a QCD leader, C.G. Fan, QCD working groups and SLD collaborators. I wish to thank T.W. Reeves and A. Weidemann for the HERWIG5.7 MC installation to SLD.

My Ph.D thesis would never been completed without the financial and spiritual support of my parents, Young and Kwang Hwang. I will not forget your love forever. I thank my wife, Kee Hyun, for her support, prayers and patience. Thanks to my son's baseball and basketball entertainment.



## TABLE OF CONTENTS

Chapter	Page
I. INTRODUCTION . . . . .	1
II. QUANTUM CHROMODYNAMICS AND THE THEORY OF THREE-JET EVENTS IN POLARIZED $Z^0$ HADRONIC DECAYS . . . . .	5
2.1 Quantum Chromodynamics . . . . .	6
2.2 Three-Jet Event Plane Orientation . . . . .	10
2.2.1 The Cross Section of Three-Jet Event . . . . .	10
2.2.2 Three-Jet Event Plane Orientation for Identified Jet . . . . .	16
2.2.3 Three-Jet Event Plane Orientation without Identifying Jet Originality . . . . .	17
2.3 Distributions of Three-Jet Scaled Energies and Ellis-Karliner Angle . . . . .	19
2.3.1 Vector Gluon Model . . . . .	19
2.3.2 Scalar Gluon Model . . . . .	21
2.4 The Hadronization and Monte Carlo Models . . . . .	22
2.4.1 Parton Showers . . . . .	23
2.4.2 The Hadronization Process . . . . .	24
2.4.3 Monte Carlo Programs . . . . .	25
2.5 Jet-Finding Schemes . . . . .	26
2.5.1 YCLUS Algorithm . . . . .	26
III. SLD AND THE SLAC LINEAR COLLIDER . . . . .	28
3.1 The SLC . . . . .	28
3.2 Polarization at SLC . . . . .	30
3.3 Overview of SLD . . . . .	32
3.3.1 Vertex Detector . . . . .	34
3.3.2 Drift Chambers . . . . .	34
3.3.3 CRID . . . . .	35
3.3.4 The Liquid Argon Calorimeter . . . . .	36
3.3.5 The Luminosity Monitor . . . . .	40
3.3.6 Warm Iron Calorimeter(WIC) . . . . .	42
3.3.7 Trigger and Data Acquisition . . . . .	42

IV. HADRONIC $Z^0$ EVENT SELECTION AND ENERGY RESPONSE CORRECTION IN THE SLD LAC . . . . .	45
4.1 Data Processing . . . . .	45
4.1.1 Trigger . . . . .	45
4.2 PASS 1 Filter . . . . .	47
4.2.1 Reconstruction . . . . .	48
4.3 Detector Simulation . . . . .	49
4.3.1 Generator Level Simulation . . . . .	49
4.3.2 Geant Simulation . . . . .	51
4.3.3 Correction of LAC Energy Response . . . . .	54
4.4 Hadronic $Z^0$ Event Selection . . . . .	59
4.5 Improved Results after LAC Energy Response Correction . . . . .	69
V. ANALYSIS AND RESULTS OF THREE-JET EVENTS IN SLD . . . . .	74
5.1 Reconstruction of Three-Jet Events . . . . .	75
5.2 Three Jets Rescaled by Momentum Conservation . . . . .	75
5.3 Comparisons of Three Jets for Hadron Particles, Corrected and Uncorrected LAC Clusters . . . . .	78
5.4 Distributions of Three-Jet Events in Raw Data and Detector Level MC . . . . .	84
5.5 Monte Carlo Simulations . . . . .	85
5.6 Corrections for Hadronization and Detector Effects . . . . .	89
5.7 The Corrected Data . . . . .	98
5.8 Systematic and Statistical Errors . . . . .	99
5.9 Results and Conclusions . . . . .	114
VI. $H^0 \rightarrow \gamma\gamma$ IN THE INTERMEDIATE HIGGS MASS AT HIGH ENERGY HADRON COLLIDERS . . . . .	116
6.1 Production of $H^0 \rightarrow \gamma\gamma$ . . . . .	117
6.2 Background Production of $H^0 \rightarrow \gamma\gamma$ . . . . .	118
6.3 How to Take the Tight Isolation Cut . . . . .	119
6.1 How to Reduce High Energetic $\pi^0$ Background . . . . .	119
VII. ANALYSIS OF A PROTOTYPE SILICON PRERADIATOR FOR HIGH ENERGY HADRON COLLIDERS . . . . .	120
7.1 Introduction . . . . .	120

	Page
7.2 Analysis of Preradiator Beam Test Results . . . . .	122
7.2.1 Pedestal Correction of Silicon Strip Detector . . . . .	124
7.2.2 Cut Conditions for Selecting Good Electron Events . . . . .	134
7.2.3 Comparison between BNL Data and MC Simulation . . . . .	140
7.2.4 Energy Resolution and Correction . . . . .	159
VIII. ANALYSIS OF LIQUID ARGON HADRON CALORIMETER PROTOTYPE FOR HIGH ENERGY HADRON COLLIDERS . . . . .	164
8.1 Introduction . . . . .	164
8.2 The Calorimeter Construction and Beam Test . . . . .	165
8.3 BNL Data and Monte Carlo (MC) Simulation . . . . .	166
8.3.1 Pedestal Distribution of BNL Data and MC Simulation . . . . .	167
8.3.2 BNL Data and MC Simulation for Arbitrary Events . . . . .	168
8.3.3 BNL Data and MC Simulation For 100 Events . . . . .	170
8.4 Energy Resolution . . . . .	178
8.4.1 Energy Resolution without the Cut Thresholds . . . . .	181
8.4.2 Energy Resolution with the Constant Cut Thresholds . . . . .	184
8.4.3 Energy Resolution with the Channel Dependent Cut Thresholds . . . . .	185
8.4.4 Comments . . . . .	185
8.5 Noise Correlation of BNL Data between Channels . . . . .	187
8.6 The Pion Rejection Studies . . . . .	188
8.7 Conclusion . . . . .	189
IX. CONCLUSION . . . . .	191
APPENDIX	
THE SLD COLLABORATION . . . . .	193
BIBLIOGRAPHY . . . . .	198

## LIST OF TABLES

Table	Page
4.1 Main Default Parameters of HERWIG5.7 Version.....	50
4.2 Correction Factors for LAC Energy Response.....	58
5.1 The Events and Statistical Errors Only of Raw Data and MC for Selected Values of $T = x_1$ in the Distribution of $\cos\theta$ , $\cos\theta_N$ and $\chi$ .....	87
5.2 Main Parameters of JETSET6.3 and JETSET7.4 which Control the Momentum Distribution of Hadrons.....	88
5.3 Statistical Errors Only of Corrections for Hadronization and De- tector Effects for $\cos\theta$ , $\cos\theta_N$ and $\chi$ Variables for Selected Values of $T = x_1$ .....	95
5.4 Statistical Errors Only of Corrections for Hadronization and De- tector Effects for $x_1$ and $x_2$ Variables.....	96
5.5 Statistical Errors Only of Corrections for Hadronization and De- tector Effects for $x_3$ and $\cos\theta_{EK}$ Variables.....	97
5.6 The Corrected Data with Experimental Systematic ( $\sigma_{sel}$ and $\sigma_{cor}$ ), Theoretical Systematic ( $\sigma_{the}$ ), Total Systematic ( $\sigma_{sys}$ ) and Statistical Errors ( $\sigma_{sta}$ ) for $x_1$ and $x_2$ .....	107
5.7 The Corrected Data with Experimental Systematic ( $\sigma_{sel}$ and $\sigma_{cor}$ ), Theoretical Systematic ( $\sigma_{the}$ ), Total Systematic ( $\sigma_{sys}$ ) and Statistical Errors ( $\sigma_{sta}$ ) for $x_3$ and $\cos\theta_{EK}$ .....	108
5.8 Experimental Systematic ( $\sigma_{sel}$ and $\sigma_{cor}$ ), Theoretical Systematic ( $\sigma_{the}$ ), Total Systematic ( $\sigma_{sys}$ ) and Statistical Errors ( $\sigma_{sta}$ ) for $\alpha$ , $\alpha_N$ and $\beta$ for Selected Values of $T = x_1$ .....	109

5.9	Parameter $\alpha$ , Statistical Error ( $d\alpha_{sta}$ ), $\chi^2$ per Degree of Freedom ( $\chi^2/ndf$ ) and Difference between $\alpha$ with Standard Cut and $\alpha$ 's with Different Cuts ( $d\alpha$ ) for Selected Values of $T = x_1$ . . . . .	110
5.10	Parameter $\alpha_N$ , Statistical Error ( $d\alpha_{Nsta}$ ), $\chi^2$ per Degree of Freedom ( $\chi^2/ndf$ ) and Difference between $\alpha_N$ with Standard Cut and $\alpha$ 's with Different Cuts ( $d\alpha_N$ ) for Selected Values of $T = x_1$ . . . . .	111
5.11	Parameter $\beta$ , Statistical Error ( $d\beta_{sta}$ ), $\chi^2$ per Degree of Freedom ( $\chi^2/ndf$ ) and Difference between $\beta$ with Standard Cut and $\beta$ 's with Different Cuts ( $d\beta$ ) for Selected Values of $T = x_1$ . . . . .	112
5.12	$\chi^2$ between Data and Vector/Scalar Gluon Predictions . . . . .	114
7.1	Run Data Information of Preradiator Beam Test. . . . .	122
7.2	Cut Conditions for Selecting Good Electrons. . . . .	141
7.3	Average Shower Profile of X and Y Strips for BNL Data. . . . .	148
7.4	Average Shower Profile of X and Y Strips for MC Simulation. . . . .	149
7.5	The Normalized Pulse Height Distribution in X Strip of BNL Data. . . . .	153
7.6	The Normalized Pulse Height Distribution in X Strip of MC Simulation. . . . .	154
7.7	One-Block Lead Glass Resolution for 5 GeV Electrons for Data and EGS Simulation. . . . .	163
8.1	Energy Resolution without Cut Thresholds. . . . .	182
8.2	Energy Resolution with Constant Cut Thresholds: Cut Threshold (60 ADC Counts). . . . .	182
8.3	Channel Dependent Cut Thresholds (Unit: ADC Counts). . . . .	183
8.4	Energy Resolution with Channel Dependent Cut Thresholds. . . . .	183

## LIST OF FIGURES

Figure	Page
2.1 Feynman Diagram for $e^+e^- \rightarrow q\bar{q}g$ at Tree Level. ....	11
2.2 Coordinate Frame in the CMS. The Three-Jet Event Plane is the x-z Plane. ....	12
2.3 The Three-Jet Event and the Ellis-Karliner Angle. ....	20
3.1 The SLAC Linear Collider (SLC). ....	29
3.2 Electron Polarization as a Function of Source Laser Wavelength. ....	31
3.3 Quadrant View of the SLD. ....	32
3.4 The SLD Vertex Detector. ....	33
3.5 The SLD Cherenkov Ring Imaging Detector (CRID). ....	35
3.6 A LAC Barrel Module. ....	37
3.7 A LAC Endcap Module. ....	38
3.8 One Cell from the Barrel LAC. ....	39
3.9 Side View of LMSAT and MASC. ....	42
3.10 Compton Polarimeter Layout. ....	44
4.1 PASS 1 Energy Sums (EHI vs. ELO). ....	48
4.2 Calorimeter Energy Response as a Function of Thrust Angle for Data. ....	50
4.3 Estimation of Material in front of the Calorimeter. ....	52
4.4 Energy Sums for Monte Carlo before PASS1 Filter (EHI vs. ELO). ....	52

4.5	The Failed Events versus $ \cos\theta_T $ after PASS1 Filter in Monte Carlo Simulation .....	53
4.6	Calorimeter Energy Response as a Function of Thrust Angle for Monte Carlo. ....	53
4.7	The Normalized Energy of Hadrons From GEANT as a Function of $ \cos\theta $ . ....	55
4.8	The Normalized Energy of Clusters in the GEANT Simulation and Data as a Function of $ \cos\theta $ . ....	56
4.9	Relative LAC Energy Response as a Function of $ \cos\theta $ . ....	57
4.10	The Correction Factor of LAC Energy Response as a Function of $ \cos\theta $ . ....	57
4.11	Total Reconstructed Energy versus Imbalance with Energy Response Correction for Data Events. ....	62
4.12	Total Reconstructed Energy versus Imbalance with Energy Response Correction for MC Hadron Events. ....	62
4.13	The Distribution of Cluster Multiplicity in the Region ( $ \cos\theta_{Thrust_{cor}}  > 0.8$ ). ....	63
4.14	The Distribution of Cluster Multiplicity in the Region ( $ \cos\theta_{Thrust_{cor}}  \leq 0.8$ ). ....	64
4.15	Total Reconstructed Energy versus Imbalance with Energy Response Correction after Hadronic $Z^0$ Selection for Data Events. ....	65
4.16	Total Reconstructed Energy versus Imbalance with Energy Response Correction after Hadronic $Z^0$ Selection for MC Hadron Events. ....	66
4.17	The Normalized Events versus Total Reconstructed Energy without Energy Response Correction after Hadronic $Z^0$ Selection for MC Hadron Events (Dashed Line Histogram) and Data (Solid Line Histogram). ....	67

4.18 The Normalized Events versus $ \cos\theta_{Thrust_{uncor}} $ without Energy Response Correction after Hadronic $Z^0$ Selection for MC Hadron Events (Dashed Line Histogram) and Data (Solid Line Histogram).....	68
4.19 LAC Energy Response as a Function of Thrust Angle for Data with Energy Response Correction. ....	68
4.20 LAC Energy Response as a Function of Thrust Angle for Monte Carlo with Energy Response Correction. ....	70
4.21 The Normalized Events versus $ \cos\theta_{Thrust} $ after Hadronic $Z^0$ Selection without Correction (Dashed Line Histogram) and with Correction (Solid Line Histogram) for Data. ....	71
4.22 The Normalized Events versus Total Reconstructed Energy after Hadronic $Z^0$ Selection without Correction (Dashed Line Histogram) and with Correction (Solid Line Histogram) for Data. ....	72
5.1 Normalized Number of Events vs. the Scaled Energies ( (A) $x_1$ , (B) $x_2$ and (C) $x_3$ ): Dashed Line Histogram (Before Correction of Momentum Conservation) and Solid Line Histogram (After Correction of Momentum Conservation.) ....	76
5.2 Normalized Number of Events vs. the Scaled Three Jets ( $x_1$ , $x_2$ and $x_3$ ) in the Difference between Hadrons at the Generator Level and Clusters at the Detector Level: Upper Part (Barrel Region) and Lower Part (Endcap Region). ....	77
5.3 Normalized Number of Events vs. Thrust and Thrust Axis Angle in the Difference between Hadrons at the Generator Level and Clusters at the Detector Level: Upper Part (Barrel Region) and Lower Part (Endcap Region).....	78
5.4 Normalized Number of Events vs. $\cos\theta_3$ and $\phi_3$ in the Difference between Hadrons at the Generator Level and Clusters at the Detector Level: Upper Part (Barrel Region) and Lower Part (Endcap Region). ....	79



5.5	Normalized Number of Events vs. $\cos\theta_1$ , $\phi_1$ , $\cos\theta_2$ and $\phi_2$ in the Difference between Hadrons at the Generator Level and Clusters at the Detector Level: Upper Part ( $\cos\theta_1$ and $\phi_1$ ) and Lower Part ( $\cos\theta_2$ and $\phi_2$ ).....	80
5.6	Normalized Number of Events vs. ( $\cos\theta$ , $\chi$ and $\cos\theta_N$ ) in the Difference between Hadrons at the Generator Level and Clusters at the Detector Level: Upper Part ( $Thrust \leq 0.9$ ) and Lower Part ( $Thrust \geq 0.9$ ).....	81
5.7	The Raw Data Distributions of $x_1$ , $x_2$ , $x_3$ , and $\cos\theta_{EK}$ Compared with Full Detector Level MC Simulation. Diamond points: Raw Data; Solid Histo: HERWIG5.7 MC Simulation at Detector Level.....	85
5.8	The Raw Data Distributions of $\cos\theta$ for Selected Values of $T = x_1$ Compared with Full Detector Level MC Simulation. Points: Raw Data; Solid Histo: HERWIG5.7 MC Simulation at Detector Level. ....	86
5.9	The Raw Data Distributions of $\cos\theta_N$ for Selected Values of $T = x_1$ Compared with Full Detector Level MC Simulation. Points: Raw Data; Solid Histo: HERWIG5.7 MC Simulation at Detector Level. ....	86
5.10	The Raw Data Distributions of $\chi$ for Selected Values of $T = x_1$ Compared with Full Detector Level MC Simulation. Points: Raw Data; Solid Histo: HERWIG5.7 MC Simulation at Detector Level. ....	87
5.11	The Parton-to-Hadron Correction Factors for $x_1$ , $x_2$ , $x_3$ and $\cos\theta_{EK}$ . ....	90
5.12	The Parton-to-Hadron Correction Factors of $\cos\theta$ for Selected Values of $T = x_1$ .....	91
5.13	The Parton-to-Hadron Correction Factors of $\cos\theta_N$ for Selected Values of $T = x_1$ . ....	91
5.14	The Parton-to-Hadron Correction Factors of $\chi$ for Selected Values of $T = x_1$ .....	92

	Page
5.15 The Hadron-to-Detector Correction Factors for $x_1, x_2, x_3$ and $\cos\theta_{EK}$ . . .	93
5.16 The Hadron-to-Detector Correction Factors of $\cos\theta$ for Selected values of $T = x_1$ . . . . .	94
5.17 The Hadron-to-Detector Correction Factors of $\cos\theta_N$ for Selected Values of $T = x_1$ . . . . .	94
5.18 The Hadron-to-Detector Correction Factors of $\chi$ for Selected Values of $T = x_1$ . . . . .	95
5.19 The Corrected 93 Data of $x_1, x_2, x_3$ and $\cos\theta_{EK}$ Distributions with <b>Statistical Error Only</b> Compared with Parton Level Simulations for Vector QCD Model and Scalar Gluon Model. . . . .	99
5.20 The Corrected 93 Data of $\cos\theta$ Distribution : $\alpha$ (the Fitting Parameter); $d\alpha$ (the <b>Statistical Error Only</b> of the Fitting Parameter) with $\chi^2$ . . . . .	100
5.21 The Corrected 93 Data of $\cos\theta_N$ Distribution: $\alpha_N$ (the Fitting Parameter); $d\alpha_N$ (the <b>Statistical Error Only</b> of the Fitting Parameter) with $\chi^2$ . . . . .	100
5.22 The Corrected 93 Data of $\chi$ Distribution: $\beta$ (the Fitting Parameter); $d\beta$ (the <b>Statistical Error Only</b> of the Fitting Parameter) with $\chi^2$ . . . . .	101
5.23 O: The Data Points of the Parameters ( $\alpha, \alpha_N$ and $\beta$ ) for Selected Values of $T = x_1$ with <b>Statistical Error Only</b> : Solid Line (Vector Gluon Theory): Dashed Line (Scalar Gluon Theory: Only VV Terms.) . . . . .	101
5.24 The Correction Factors of LAC Energy Response: Solid Line: $0.9 \times$ Correction Factor for $\cos\theta > 0.69$ and Dashed Line: $1.1 \times$ Correction Factor for $\cos\theta > 0.69$ . . . . .	104
5.25 The Systematic Errors from Various Sources for $x_1, x_2, x_3$ and $\cos\theta_{EK}$ . . . . .	106
5.26 The Systematic Errors from Various Sources for $\alpha, \alpha_N$ and $\beta$ . . . . .	106

5.27	The Corrected 93 Data of $x_1$ , $x_2$ , $x_3$ and $\cos\theta_{EK}$ Distributions with <b>Total Errors</b> Compared with Parton Level Simulations for Vector QCD Model and Scalar Gluon Model. ....	109
5.28	Parameters ( $\alpha$ , $\alpha_N$ and $\beta$ ) with <b>Total Errors</b> for Selected Values of $T = x_1$ : Solid Line (Vector Gluon): Dashed Line (Scalar Gluon).....	113
5.29	Comparison between the Corrected Data of LAC and the Corrected Data of CDC: $\times$ (Corrected Data of LAC with <b>Total Errors</b> ): $\diamond$ (Corrected Data of CDC with <b>Statistical Errors Only</b> ). ....	113
5.30	$\cos\theta_N$ Depending on Right or Left Helicities of an Electron Beam Polarization 63% during 93 Run with <b>Statistical Errors Only</b> : Hist (Left Helicity) and O (Right Helicity) .....	115
7.1	Pulse Height Distributions for all 96 Strips under Different Conditions: (a) Upper-Left (Pedestals Only); (b) Upper-Right (5 GeV Electrons with No Radiator); (c) Lower-Left (1 $X_0$ of Tungsten); (d) Lower-Right (3 $X_0$ of Tungsten). ....	123
7.2	Uncorrected Pulse Height versus Strips: Unit of Pulse Height is ADC Counts. ....	125
7.3	Correlative Relations for Arbitrary Channels (14, 20,25,30,35,48) vs. Reference Channel (9) for the Uncorrected Pedestals. ....	125
7.4	Correlative Relations for Arbitrary Channels (14, 20,25,30,35,48) vs. Reference Channel (48) for the Uncorrected Pedestals. ....	126
7.5	Correlative Relations for Arbitrary Channels (14, 20,25,30,35,48) vs. Reference Channel (57) for the Uncorrected Pedestals. ....	126
7.6	Correlative Relations for Arbitrary Channels (14, 20,25,30,35,48) vs. Reference Channel (96) for the Uncorrected Pedestals. ....	127
7.7	Correlative Relations for Arbitrary Channels (14, 20,25,30,35,48) vs. Reference Channel(97) for the Uncorrected Pedestals.....	128

7.8	Correlative Relations for Arbitrary Channels (14, 20,25,30,35,48) vs. Reference Channel (97) for the Corrected Pedestals. ....	129
7.9	The Sum of all Events and all Channels versus Pulse Heights: (a) Uncorrected Data (Upper-Left), (b) Uncorrected Pedestal (Upper-Right), (c) Corrected Data (Lower-Left), (d) Cor- rected Pedestal (Lower-Right).....	132
7.10	Corrected Pulse Height versus Strips: Unit of Pulse Height is ADC Counts. ....	133
7.11	Distribution of Deposited Energy Taken at Center Block of Lead Glass. ....	133
7.12	Left: a $3 \times 4$ Block Array of Lead; Right: The Silicon Strip Detector. ....	135
7.13	The Normalized High and Low Asymmetry of Lead Glass ver- sus Channel of Maximum Pulse Height in X Silicon Strip Detector.....	135
7.14	The Normalized Left and Right Asymmetry of Lead Glass versus Channel of Maximum Pulse Height in Y Silicon Strip Detector. ....	136
7.15	The Sum for all Events of Pulse Height Greater than 15 ADC as a Function of Strip Number. ....	139
7.16	The Distribution of Difference between X and Y Cluster Values. ....	139
7.17	Event Displays of Data for the First 6 Events of a Run with 5 GeV Electrons and 3 $X_0$ of Tungsten. These Displays Give Pulse Height (Measured Charge in ADC Counts) versus Strip Number. ....	142
7.18	Event Displays of MC Simulated with 5 GeV Electrons and 3 $X_0$ of Tungsten: These Displays Give Pulse Height (Measured Charge in KeV Counts) versus Strip Number.....	143
7.19	Pulse Height Distribution of MC Pedestal Simulated with Corrected Pedestal Data. ....	143

7.20	Event Displays of MC with Added Noise Effect. ....	144
7.21	Data (2862 Electron Events). Upper Row Describes X Strips: Left (Sum of Pulse Heights of all Events), Middle (Sum of all Events), and Right (Average Value) as a Function of Channels): Bottom Row Describe Y Strips: Left, Middle, and Right Same as X strips. ....	146
7.22	MC (100 Simulation Events). Upper Row Describes X Strips: Left (Sum of Pulse Heights of all Events), Middle (Sum of all Events), and Right (Average Value) as a Function of Channels): Bottom Row Describe Y Strips: Left, Middle, and Right Same as X strips. ....	147
7.23	Pulse Height Distribution of 8 Strips (17-24) of X Strips for all Events: The Average of MIPs is about 8.5 ADC Counts. ....	150
7.24	The Normalized Pulse Height Distributions of Each Channel (-3 to 2) around the Channel of Maximum Pulse Height at MC Simulation (100 Events). ....	151
7.25	The Normalized Pulse Height Distributions of Each Channel (-3 to 2) around the Channel of Maximum Pulse Height at Data (2862 Events). ....	152
7.26	Transverse Shower Profile for X Strips Averaged 2862 Events for 5 GeV Electrons with $3 X_0$ of Tungsten Radiator (Squares). The Histogram is the Corresponding EGS Simulation for 100 Events. ....	153
7.27	Transverse Shower Profile for Y Strips Averaged 2862 Events for 5 GeV Electrons with $3 X_0$ of Tungsten Radiator (Squares). The Histogram is the Corresponding EGS Simulation for 100 Events. ....	154
7.28	Distribution of Number of Strips over Threshold as a Function of that Threshold for Data and EGS Simulation in X Strips. ....	156
7.29	Distribution of Number of Strips over Threshold as a Function of that Threshold for Data and EGS Simulation in Y Strips. ....	157

7.20	Summation of all Events versus Pulse Height (ADC Counts) for BNL Data for the Good 2862 Events.....	157
7.31	Summation of all Events versus Pulse Height (ADC Counts) for MC for the 100 Simulation Events. ....	158
7.32	Scatter Plot of Total Measured Silicon Energy versus Measured Lead Glass Energy. The Line Indicates the Fitted Correlation between These Quantities. ....	159
7.33	The Corrected Energy Resolution of $3 X_0$ of Tungsten for the Minimization Method for Data. ....	161
7.34	The Uncorrected Energy Resolution of Central Lead Glass for $3 X_0$ Tungsten Data. ....	161
7.35	The Energy Resolution of Central Lead Glass with No Preradiator Data.....	162
7.36	The Energy Resolution of Central Lead Glass with No Preradiator MC Simulation.....	162
8.1	Side View of Layers in the Calorimeter Module. ....	166
8.2	Signal Boards for the Calorimeter. ....	167
8.3	Pedestal Distribution of 10 GeV $\pi^-$ with 430 Events. ....	168
8.4	MC simulation with Condition of Pedestal Distribution of 10 GeV $\pi^-$ . ....	169
8.5	Pedestal Distribution of BNL Data in Summation of all 240 Strips with an Average of 46 ADC Counts and a Standard Deviation of 428 ADC Counts with 584 Events. ....	169
8.6	MC Distribution in Summation of all 240 Strips with an Average 37 ADC Counts and a Standard Deviation of 432 ADC Counts with 1,000 Events. ....	170

8.7	The Deposited (Signal + Pedestal) Energies versus Strips in Each Stack for an Arbitrary Event (BNL Data for 10 GeV $\pi^-$ ).....	171
8.8	The Pedestal Energies versus Strips in Each Stack for an Arbitrary Event (BNL Data for 10 GeV $\pi^-$ ). .....	172
8.9	The Simulated (Signal) Energies versus Strips in Each Stack for an Arbitrary Event (MC Simulation for 10 GeV $\pi^-$ ). .....	173
8.10	The Simulated (Signal + Pedestal) Energies versus Strips in Each Stack for an Arbitrary Event (MC Simulation for 10 GeV $\pi^-$ ). .....	174
8.11	The Deposited (Signal + Pedestal) Energies versus Strips in Each Stack for Arbitrary Events (BNL Data for 10 GeV $\pi^-$ ).....	175
8.12	The Simulated (Signal) Energies versus Strips in Each Stack for Arbitrary Events (MC Simulation for 10 GeV $\pi^-$ ).....	176
8.13	The Simulated (Signal+Pedestal) Energies versus Strips in Each Stack for Arbitrary Events (MC Simulation for 10 GeV $\pi^-$ ). .....	177
8.14	The Distribution of the 20 GeV $\pi^-$ Energies of BNL Data without Cut Threshold for 1,000 Events with the Overlaid Gaussian.....	178
8.15	Energy Distributions for Constant Cut Thresholds of 30, 40, 50, 60, 70 and 80 ADC Counts for 1,000 Events in BNL Data of 20 GeV $\pi^-$ .....	179
8.16	Signal Energy Distribution for Four Different Regions of the First Stack: Upper-Left is Edge, Upper-Right is Intermediate Center, Lower-Left is Intermediate Edge and Lower Right is Center. ....	180
8.17	Noise Distribution for Four Different Regions of the First Stack: Upper-Left is Edge, Upper-Right is Intermediate Center, Lower-Left is Intermediate Edge and Lower Right is Center. ....	180

8.18 Energy Distribution of BNL Data of 20 GeV $\pi^-$ with Channel Dependent Cut Thresholds for 1,000 Events. ....	181
8.19 Noise Correlation between Channels for Six Channels from the First (Upper-Left) to the Sixth Channel (Lower-Right). ....	187
8.20 Rejection Factor versus Cut Energy (ADC Counts). ....	188